Received: 31 January 2020 | Revised: 22 April 2020 | Accepted: 23 April 2020

DOI: 10.1002/jrs.5897

Check for updates

SPECIAL ISSUE - RESEARCH ARTICLE

Journal of RAMAN SPECTROSCOPY WILEY

Studies of supercontinuum generation in a photonic crystal fiber for use as Stokes beam in a single-laser femtosecond micro-CARS setup

Serena Gagliardi | Michele Marrocco | Flaminia Rondino | Domenico Palumbo | Caterina Merla | Mauro Falconieri

ENEA, C. R. Casaccia, Rome, Italy

Correspondence
Mauro Falconieri, ENEA, C.R. Casaccia, via Anguillarese 301, 00123 Rome, Italy.
Email: mauro.falconieri@enea.it

Funding information
ENEA

Abstract

Photonic crystal fibers (PCFs) have gained popularity thanks to the use of their broad and efficient supercontinuum (SC) emission as Stokes source in ultrafast multiplex coherent anti-Stokes Raman scattering microscopy. Here, the infrared portion of the SC emitted by a widely used PCF is studied in a basic CARS experiment with a single laser oscillator operated at various conditions of power and chirp values. The dependence of the SC and CARS signal of reference cyclohexane sample on the operative conditions of the laser is examined and illustrated by means of statistical approaches that serve the purpose of defining and quantifying the reliability of CARS measurements in relation to the characteristic of the Stokes pulse coming from the fiber. Statistical techniques based on principal component analysis, on calculation of statistical momenta of the SC spectra, and on Allan variance studies are introduced to help to identify the best working regime. Principal component analysis was used to quantify the correlation of SC spectra with PCF input power, which is found to be stronger at high laser beam chirp values. First and second momenta of SC spectra allow identification of best operating conditions with respect to peak emission wavelength and spectral width. Finally, the behavior of Allan variance shows that the time stability of Stokes and CARS signals clearly depends on the chirp of the pump pulse, evidencing that high chirp conditions correspond to lower variance values at the expense of stability for longer measurement times.

KEYWORDS

femtosecond CARS, multiplex CARS, photonic crystal fiber, principal component analysis, supercontinuum generation

1 | INTRODUCTION

Applications of coherent anti-Stokes Raman scattering (CARS) as a vibrational imaging tool[1,2] are presently subject of intensive investigation, and novel experimental configurations are reported to reduce cost and complexity of the apparatus while improving the system performances to address specific issues. In particular, systems equipped with a single femtosecond laser oscillator in the so-called multiplex CARS configuration have been

 © 2020 John Wiley & Sons, Ltd.

demonstrated to be very interesting for biomedical applications because of their capability of hyperspectral imaging with energies adequate for interaction with biological samples[3–6] at reduced costs and complexity.

In femtosecond multiplex CARS, the beam from an ultrafast oscillator, usually a self-Kerr lens modelocked Ti:sapphire laser, is split to provide both the degenerate pump/probe pulses and the Stokes pulses, the latter being the supercontinuum (SC) light originated in a highly nonlinear photonic crystal fiber (PCF). The pulses are then overlapped spatially and temporally and routed to the sample using a microscope whose objective delivers the necessary fluence to produce the nonlinear interaction. The CARS signal is then collected either in forward scattering with a second objective or in backward (epi) configuration.[7,8]

In view of optimized and reliable operation of such a system, control of the behavior of the PCF is an important step. Indeed, the SC spectral distribution determines the accessible vibrational bandwidth, its chirp controls the system spectral focusing capability, and its noise and stability determines the CARS imaging acquisition rate and overall performances.[9–11]

Several studies are available in the literature on SC generation in PCF for uses in single-oscillator femtosecond CARS application, employing initially fibers with a single zero-dispersion wavelength (ZDW) near the excitation wavelength,[12] and subsequently the more recent fibers designed to possess two nearby ZDWs.[13–15] Reasons for the advent of these new PCFs are related to the idea that phase-matching condition, needed for the nonlinear processes to occur within the fiber, can be achieved at any wavelength between the ZDW extremes.[13] Understandably, this allows a wide range of choice for the combination of pump and Stokes frequencies. Later investigations[16,17] have compared the behavior of different PCFs, with closely or far-lying two ZDW, also identifying latent spectral artifacts due to polarization-dependency of the SC emission, showing that, when the working conditions are properly chosen, they are both suitable for use in CARS systems.

These studies evidence the importance of selecting proper PCF excitation conditions (i.e., laser beam power, wavelength, and chirp) to achieve optimal SC spectral distribution and minimal noise[14,18–21] and therefore better performances for CARS measurements.[17,22] Numerical modelling[13,18,23] can be of help to this aim and has been actually used to simulate the SC generation, proving successful in reproducing the gross features of the experimental SC spectra and to evaluate optical noise,[24,25] even though detailed agreement with experimental data can be obtained at the expense of purposely introduced adjustments of the input parameters.[22] As far as noise and instabilities are concerned, it has been reported that noise in the SC spectra has two components[14,25]: the first, at high frequency, is related to the shot noise and has been widely investigated both theoretically and experimentally,[13,14,16,24,25] and a second, at low frequency, referred to as technical noise, which is due to amplification of the fluctuations of the input pulse characteristics. The latter, albeit the care taken in the experimental setup and working conditions, is anyway present and unavoidable.[25,26] Moreover, another point which deserves attention is the sensitivity of the SC beam to unavoidable thermal and mechanical instabilities which degrade the fiber coupling efficiency, leading to variations of the SC spectral distribution within the time scale of several seconds. Unless active feedback systems are used to stabilize the PCF coupling,[12] these instabilities must be taken into account for practical use of SC beams in CARS systems, even though their actual time scale and extent is somewhat dependent on the setup details and ambient conditions. Indeed, the behavior of the SC beam is due to the interplay between the selected PCF excitation conditions and the coupling instabilities, because the formers determine the sensitivity to misalignment.

Given the difficulty to systematically describe this interplay, here, we propose a statistical approach for the characterization of the SC beam. The attempt is made to find the optimal working point of a widely used commercially available PCF (FemtoWHITE CARS®) with two nearby ZDWs with respect to both the excitation conditions and alignment drift. By repeated measurements of the SC spectra in different excitation conditions, and using statistical descriptors, we were able to evidence nontrivial relationships between the SC spectra shape and stability and the input beam power and chirp, reducing the importance of the substantial spectral variations determined by the coupling instabilities. Following this line of research, we also show the effect of the input beam chirp and pulsewidth on the long-term (tens to hundreds of seconds) stability of the Stokes beam and of the CARS signal studied by means of the Allan variance statistical descriptor.[27,28] Fluctuations on this timescale are relevant for long-time measurements such as those necessary for acquisition of extended CARS maps or for the study of kinetic processes.

2 | EXPERIMENTAL

2.1 | Optical setup

The experimental setup used in this work is derived from the one described in detail in Falconieri et al.[22] with

some minor modifications, and is shown in Figure 1. Briefly, the pulses emitted at 780 nm by an ultrafast Ti: sapphire oscillator (Coherent MIRA-900F) operating at 76 MHz rep. rate are divided in two beams by a 50/50 beam splitter, one portion being coupled to a FemtoWHITE CARS® PCF (NKT Photonics) by a 40× objective to provide the SC for the Stokes beam, and the other being used to provide the pump/probe beam. Typical PCF coupling efficiencies were measured to be around 40%. The SC produced by the PCF is recollimated by a 20× objective, filtered by a 750-nm long-wave pass filter and recombined with the pump/probe beam by a dichroic mirror (Semrock LP02-780RU-25 RazorEdge®), whereas the temporal superposition of the pulses of the two beams is achieved by a delay line placed on the pump/probe arm. The bandwidth of this beam is reduced by a narrow bandpass filter (Semrock LL01-780-25 MaxLine®) to improve the CARS resolution. A small portion of the SC beam is routed to a mechanical chopper and to a monochromator/InGaAs detector assembly to measure the Stokes beam spectrum using a lock-in amplifier; typical measurement time of a spectrum was around 30 s. The Stokes and pump/probe beams are focused onto the sample by a long working distance 32× objective (Leitz Wetzlar), and the CARS signal is collected by a 20× (Leitz Wetzlar) objective in forward configuration. The signal is filtered by an edge filter (Semrock SP01-785RU-25 RazorEdge®) and launched into a fiber to be delivered to a monochromator/detector assembly composed by a Horiba/Jobin Yvon TRIAX 320 monochromator and by an Andor Newton intensified CCD. In this work, the CARS signal was measured on a cyclohexane sample contained in a quartz cuvette. Attempts at CARS imaging were not made because imaging is not necessary for the problem in hand and would add further complications.

Part of this work is devoted to the study of the influence of coupling instabilities, and care was thus taken to improve the solidity of the setup. In particular, the distance L between the fiber and the laser is kept at minimum ($L = 60$ cm), and the whole setup is mounted on a 30-cm-thick TMC optical table kept in a laboratory with controlled temperature to ±0.5°C. The fiber, the launching, and recollimation objectives are mounted on a Thorlabs Nanomax® flexure stage providing three-axis adjustment with differential actuators.

2.2 | Control of PCF excitation conditions

The PCF input average power and chirp were varied by adjusting a variable attenuator and the laser intracavity prism compressor, respectively. The laser pulse chirp is quantified here by the chirp parameter R defined as the ratio of the measured time-bandwidth product (TBP) to that of transform-limited pulses, that is, 0.315 for sech^2 pulses.[29] The pulse duration τ and the FWHM bandwidth Δf were measured at the laser exit port for each position of the laser intracavity prism using an autocorrelator (APE PulseCheck) and a monochromator-CCD assembly respectively. Typical attained laser pulse dispersion properties are shown in Table 1, where it can be seen that adjustment of the intracavity prism compressor allowed attainment of pulses whose TBP ranges from

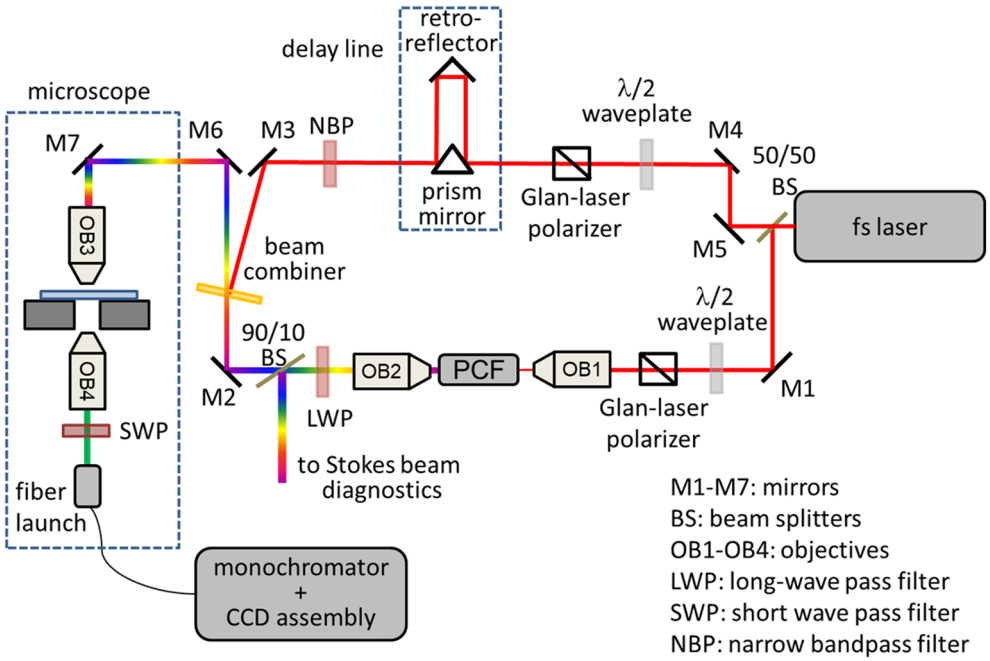

FIGURE 1 Experimental layout of single-laser-oscillator multiplex CARS

TABLE 1 Typical values of the laser beam pulsewidth and chirp parameter *R*, defined as ratio of pulse time-bandwidth product to transform-limited value (0.315), obtained by changing the amount of dispersion introduced by the laser intracavity prism compressor

Laser pulsewidth FWHM (fs)	Chirp parameter *R*
136	1.56
113	1.62
102	1.65
95	1.76
87	1.97

1.5 to 1.9 times the transform-limited value. The beam chirp at the fiber input is determined by the initial chirp of the laser added to the contribution coming from dispersion of the optical components. In our setup, the only sensible contribution is given by the second-order dispersion of the launching objective, which was estimated to be approximately equal to about 1250 fs^2 by measuring the pulse duration before and after the objective. In the following, we will only refer to the effect of the laser beam chirp because the objective contribution is constant throughout this work.

2.3 | Data analysis

In the first part of the experiment, we studied the dependence of the Stokes beam on the excitation conditions by measuring the infrared part of the SC spectrum five times for each power and chirp condition. The fiber coupling was carefully re-aligned each time between measurements by maximizing the output power. Nevertheless, the experimental spectra were found to be not completely reproducible and were therefore analyzed statistically to bring out the common features. To this end, principal component analysis (PCA) was first employed, as implemented using a MATLAB® code. Without going into the details, we recall that in this analysis method,[30] each spectrum, composed by *n* couples [λ, *I*(λ)], after subtraction of the mean value of the data ensemble for each wavelength[31] (mean centering), is first represented as a point whose coordinates are the intensities at each measured wavelength in a *k*-dimensional space, *k* being the minimum value between *n*-1 and the number of spectra. In this representation, spectra with similar intensities and shape are grouped into clusters, and the directions which maximize the data variance between clusters define the principal components of the data set, which constitute a new coordinate system (the first principal component pertaining to the direction of largest variance of the data, and the other components to decreasing values of variance). The coordinates of the experimental points along the new coordinate system can be put in relationship with the experimental parameters using statistical methods,[30] so that the correlation between these parameters and the spectra features can be sorted out. Furthermore, the correlation among spectra variables, that is, the measurement wavelengths, and their influence on the principal components can be estimated using the so-called loading plot, where the spectra variables are represented in the principal components coordinate system.

In addition to the PCA approach, the first and second moment of the intensity distribution of the spectra, that is, their center-of-mass (COM), and their spectral width, or standard deviation around the COM, were calculated to derive global descriptors of the spectra related to the PCF excitation conditions.

In the second part of the experiment, the long-term fluctuations of the Stokes beam and of the CARS signal, and their correlation, were studied as a function of the laser beam chirp conditions using the Allan variance description[27] according to the prescriptions given in Ossenkopf.[28] In particular, the intensity of the CARS signal of cyclohexane at 633 nm (corresponding to a Raman shift equal to 2,978 cm^{-1}) and the related Stokes intensity at 1,016 nm were repeatedly measured at fixed time intervals of 30 s for 20 min, with 0.5-s measurement time in different laser beam chirp conditions.

3 | RESULTS AND DISCUSSION

The infrared parts of several SC spectra collected under different excitation power and beam chirp were analyzed using the principal component analysis. To contain the length of this paper and to avoid weighing it down with too many figures, PCA plots for all the data sets used in this study are reported in Figure S1.

PCA shows (see Figure S1) that in our case, the first component (PC1) accounts for a substantial fraction of the spectral variations and results to be strongly correlated with the PCF input peak power as shown in Table 2 for each chirp condition. This is actually expected and in agreement with calculations and experiments[13,14] showing substantial SC spectral changes in dependence of the fiber input power.

Unfortunately, our attempts to identify the experimental parameter(s) correlated with the second principal component (PC2), which however accounts for a reduced part of the spectral variations, were not successful, and the nature of this component will be subject of further investigations. The result evidenced by PCA analysis and shown in Table 2 is that for shorter pulses and higher

TABLE 2 Percentage of explained variance of the first two principal components, and correlation of first principal component with the fiber input peak power for different laser beam chirp conditions

Chirp parameter *R*	PC1%	PC2%	PC1 correlation with peak power (Pearson coefficient)
1.56	70.52	9.28	0.86
1.62	54.45	15.08	0.84
1.65	81.06	8.21	0.95
1.76	82.02	8.58	0.88
1.97	88.56	5.82	0.96

chirp parameters the SC spectra dependence on the input power is higher than in other conditions. Noticeably, the greater the correlation of the SC spectrum with the PCF input power, the lesser the importance of other possibly uncontrolled parameters such as spatial chirp, higher order dispersion, and so on. PCA can give further insight into the behavior of the PCF when considering the loading plots (see Figure S2) where the spectra variables (measurement wavelengths) are shown on the PC1-PC2 coordinate system. According to the above analysis, the wavelengths lying along the first principal component are strongly correlated with the PCF input power and can be considered as predictable lines, because the intensity of the emission is in practice univocally determined by the input power. On the other hand, spectral emissions depending on the second principal component are not strictly determined by the input power so they may be considered more prone to fluctuations.

The distinction between these two sets of spectral components is somewhat arbitrary and here we assign to the first set the wavelengths having the projection on the PC1 component greater than four times the projection on PC2 in the PC1-PC2 Cartesian plane. These wavelengths are shown in Figure 2 together with the averages of the SC spectra measured under different laser beam chirp conditions at maximum PCF input power.

Some of the wavelengths evidenced in Figure 2 correspond to low intensity regions of the SC spectra, so that their dependence on PC1 represents a power dependent background emission not very relevant for CARS measurement. Differently, wavelengths with strong PC1 loading placed at, or near, SC emission peaks are useful, and can be interpreted as predictable and controllable components of the spectrum. For the lower and higher laser beam chirp values a greater number of "reliable" wavelengths, belonging to a wider spectral region, is evidenced, pointing out for a possibly wider spectral region where the SC intensity is controllable by the PCF input power. A dependence of the technical noise on the SC wavelength and on the laser excitation chirp is also shown in Newbury et al.[26] even though the latter dependence is weak due to the reduced chirp range explored in that paper.

The global properties of the SC spectra as function of input power and beam chirp parameter *R* can also be discussed in terms of their center-of-mass (COM) and spectral width, or standard deviation about the COM, as shown in Figure 3a,b, respectively.

From Figure 3a, it can be seen that, as expected, the COM of all spectra shifts to longer wavelengths for increasing power but longer wavelengths are obtained at

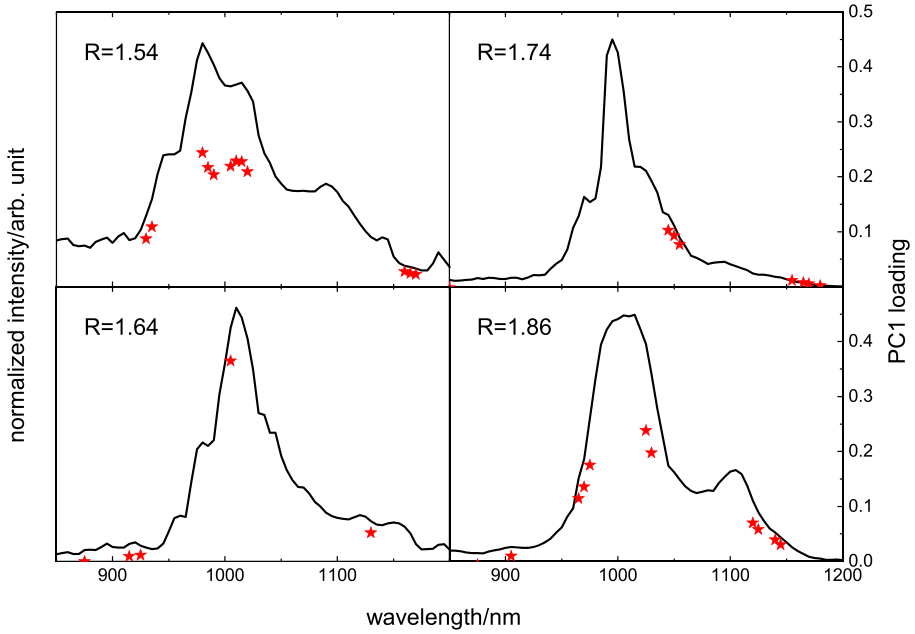

FIGURE 2 Averaged infrared portions of the SC spectra measured at maximum fiber input power (continuous line) as a function of the excitation beam chirp parameter *R*, and wavelengths with maximum loading (see text) on PC1 (stars)

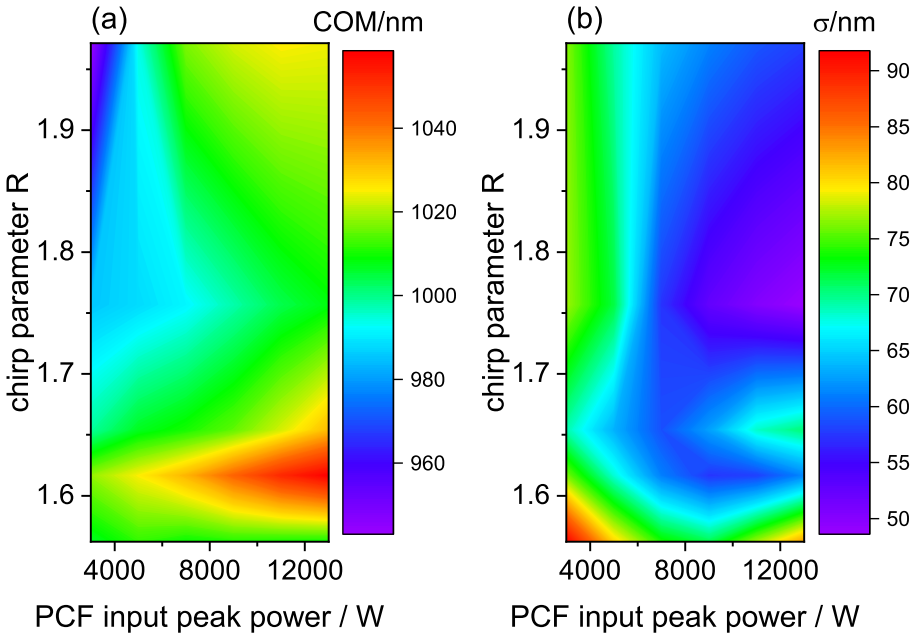

FIGURE 3 Center of mass (COM) (a) and standard deviation about COM (b) of the Stokes beam as function of laser beam chirp parameter *R*, and PCF input peak power

low chirp values. The power dependence of the COM is stronger for the lower and higher chirp values, although is somewhat reduced at intermediate values. This confirms the above interpretation of the PCA results because a broader SC spectral region is scanned when the PCF input power is varied.

The width of the SC spectra, as shown in Figure 3b, is larger for low chirp values, which is interesting for multiplex CARS operation. The existence of an optimum chirp value maximizing the SC bandwidth was also theoretically predicted in Zhu and Brown.[21] The prominence of a well-defined band is evidenced by reduced standard deviation figures and is attained at intermediate values of chirp and power, which is of interest for CARS measurements at fixed Raman shifts. In particular, the lowest standard deviations values are obtained in the medium- to high-power, intermediate chirp region, associated with a COM wavelength around 1,000 nm.

The Allan variances of the intensity of the Stokes beam and of the CARS signal of a cyclohexane sample

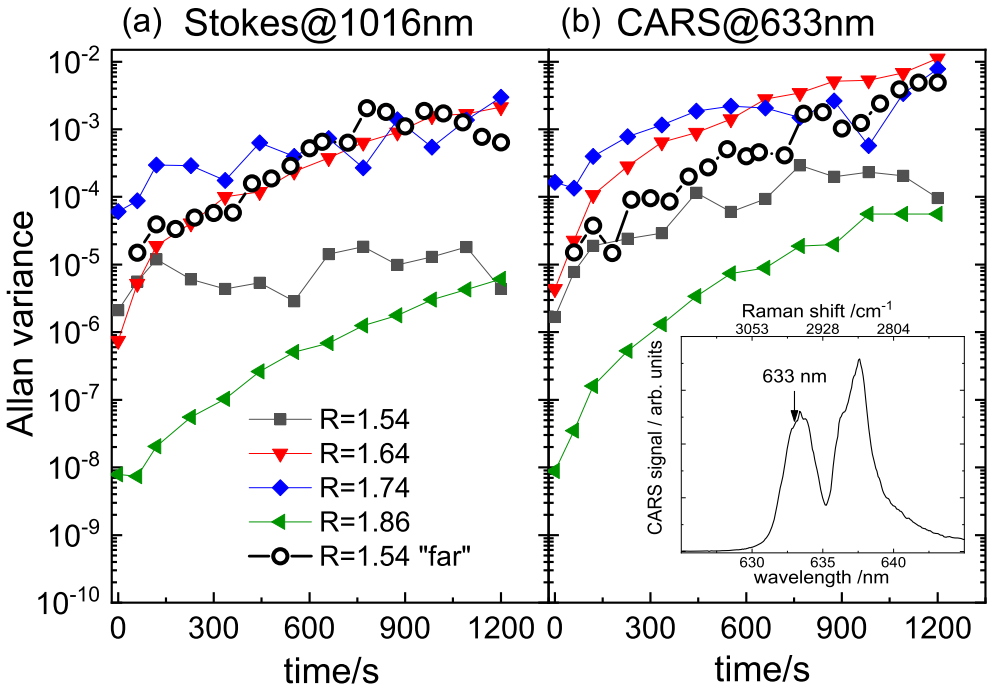

FIGURE 4 Allan variances of the Stokes beam intensity at 1,016 nm (a) and of the CARS signal of cyclohexane at 633 nm (b), for different values of the laser chirp parameter *R*. Also shown the Allan variances for $R = 1.54$ calculated for signals measured in a setup with longer optical path from the laser exit port to the PCF launching objective (165 cm), (open circles "far"). Inset: CARS spectrum of cyclohexane

measured at 1,016 and 633 nm, respectively, in different laser beam chirp conditions are reported in Figure 4, together with the CARS spectrum of cyclohexane (inset).

As a general trend, the Allan variances increase as function of time, showing the effect of the long-time instabilities. The Allan variance of the CARS signal follows the Stokes beam one with an excess contribution due to noise added by the interaction with the pump/probe beam. A dependence on the laser beam chirp is also apparent. This underlines again the interplay between PCF excitation conditions and the performances of the setup. At the higher chirp value, the Allan variance of Stokes and CARS signals is definitely smaller but less stable (green solid triangles), an optimal condition for short-time measurements. With increasingly smaller chirps (red solid triangles and blue solid diamonds), values are greater whereas the time correlation improves. The smallest chirp (black solid squares) results in lower noise contributions with values between the observed extremes. So the latter condition seems suitable for extended time measurements such as kinetic studies or large vibrational maps of weak signals. One additional feature of Figure 4 is visible in the comparison between the evolutions at $R = 1.54$ obtained for two experimental configurations distinguished by the different length of the optical path L going from the laser oscillator to the PCF launching objective (open circles: $L = 160$ cm, solid squares: $L = 60$ cm). As expected, the Allan variance for the longer optical path shows the presence of increased noise contributions, evidencing the importance of a well-designed setup for optimal system performances.

4 | CONCLUSIONS

In conclusion, we have first studied the effects of PCF excitation conditions, as input peak power and beam chirp, on the infrared portion of the generated SC spectrum, pointing out the interplay between the spectrum stability and the fiber working point. To this aim, we have described the features of the SC spectrum by statistical methods, thus reducing the importance of fluctuations due to coupling instabilities occurring in any real system. Principal component analysis shows that laser power is the primary component responsible for the shape of the whole infrared Stokes distribution. This is confirmed at various chirp values by analysis of SC spectra center of mass and width, showing that the power dependence of the spectra COM is stronger for the lower and higher chirp values although is somewhat reduced at intermediate values, whereas longer emission wavelengths are obtained at low chirp values. PCA secondary components are of minor importance but attempts at identifying them were unsuccessful at the time of this submission. Allan variance method, used to study the long-time fluctuations of the Stokes beam at fixed frequency and of the corresponding CARS signal measured on a reference sample, leads us to conclude that low and high laser chirp values provide best conditions for short and long measurement times, respectively. Thus, in this work, the influence of the laser beam chirp and power on both the PCF stability and CARS signal is experimentally evidenced and characterized, providing useful information for the selection of the fiber working point in view of optimized CARS system operation. It is reasonable to assume that our findings are mainly determined by the PCF and laser oscillator behavior. So, given the almost standardized use of the FemtoWHITE CARS PCF and of self-Kerr lens modelocked oscillators with intracavity dispersion compensation prisms in femtosecond micro-CARS setups, we expect our findings to be of general applicability.

ACKNOWLEDGEMENTS

This work was performed within the LINC (Laboratory for Interdisciplinary CARS Spectroscopy) project, funded by ENEA DTE, FSN, and SSPT Departments and by DTE-PCU, FSN-TECFIS, and SSPT-TECS Divisions, whose financial support is gratefully acknowledged.

ORCID

Michele Marrocco https://orcid.org/0000-0002-5279-9497

Mauro Falconieri https://orcid.org/0000-0001-5184-4834

REFERENCES

[1] A. Zumbusch, G. R. Holtom, X. S. Xie, *Phys. Rev. Lett.* **1999**, *82*, 4142.
[2] C. L. Evans, X. S. Xie, *Annu. Rev. Anal. Chem.* **2008**, *1*, 883.
[3] A. M. Zheltikov, *J. Raman Spectrosc.* **2000**, *31*, 653.
[4] F. Pegoraro, A. D. Slepkov, A. Ridsdale, J. P. Pezacki, A. Stolow, *Appl. Optics* **2010**, *49*, F10.
[5] A. C.-T. Ko, L. B. Mostaço-Guidolin, A. Ridsdale, A. F. Pegoraro, M. S. D. Smith, A. Slepkov, M. D. Hewko, E. K. Kohlenberg, B. Schattka, A. Stolow, M. G. Sowa, *Proc. SPIE* **2011**, *7903*, 790318.
[6] J. G. Porquez, R. A. Cole, J. T. Tabarangao, A. D. Slepkov, *Opt. Lett.* **2017**, *42*, 2255.
[7] J.-X. Cheng, Y. K. Jia, G. Zheng, X. S. Xie, *Biophys. J.* **2002**, *83*, 502.
[8] A. Volkmer, J.-X. Cheng, X. S. Xie, *Phys. Rev. Lett.* **2001**, *87*, 023901.
[9] R. A. Cole, A. D. Slepkov, *J. Opt. Soc. Am. B* **2018**, *35*, 842.
[10] B.-C. Chen, J. Sung, X. Wu, S.-H. Lim, *J. Biomed. Opt.* **2011**, *16*, 021112.
[11] S. Michel, A. Courjaud, E. Mottay, C. Finot, J. Dudley, H. Rigneault, *J. Biomed. Opt.* **2011**, *16*, 021108.

[12] C.-H. Hage, B. Kibler, E. R. Andresen, S. Michel, H. Rigneault, A. Courjaud, E. Mottay, J. M. Dudley, G. Millot, C. Finot, *Proc. SPIE* **2011**, *8071*, 80710I.
[13] K. M. Hilligsøe, T. V. Andersen, H. N. Paulsen, C. K. Nielsen, K. Mølmer, *Opt. Express* **2004**, *12*, 1045.
[14] S. Murugkar, C. Brideau, A. Ridsdale, M. Naji, P. K. Stys, H. Anis, *Opt. Express* **2007**, *15*, 14028.
[15] M. H. Frosz, P. Falk, O. Bang, *Opt. Express* **2005**, *13*, 6181.
[16] M. Naji, S. Murugkar, H. Anis, *Opt. Express* **2014**, *22*, 10800.
[17] J. G. Porquez, R. A. Cole, A. D. Slepkov, *OSA Continuum* **2018**, *1*, 1385.
[18] J. Vengelis, V. Jarutis, V. Sirutlkalis, *Optim. Eng.* **2018**, *57*, 016102.
[19] X. Hu, Y. Wang, W. Zhao, Z. Yang, W. Zhang, C. Li, H. Wang, *Appl. Optics* **2010**, *49*, 4984.
[20] X. Fu, L. Qian, S. Wen, D. Fan, *J. Opt. A: Pure Appl. Opt.* **2004**, *6*, 1012.
[21] Z. Zhu, T. G. Brown, *Opt. Express* **2004**, *12*, 689.
[22] M. Falconieri, M. Marrocco, C. Merla, S. Gagliardi, F. Rondino, M. Ghezelbash, *J. Raman Spectrosc.* **2019**, *50*, 1287.
[23] J. Dudley, R. Taylor, *Supercontinuum Generation in Optical Fibers*, Cambridge University Press, New York **2010** Chap. 3.
[24] J. M. Dudley, S. Coen, *Opt. Lett.* **2002**, *27*, 1180.
[25] K. L. Corwin, N. R. Newbury, J. M. Dudley, S. Coen, S. A. Diddams, K. Weber, R. S. Windeler, *Phys. Rev. Lett.* **2003**, *90*, 113904.
[26] N. R. Newbury, B. R. Washburn, K. L. Corwin, R. S. Windeler, *Opt. Lett.* **2003**, *28*, 944.
[27] D. W. Allan, *IEEE Proc.* **1966**, *54*, 221.
[28] V. Ossenkopf, *Astron. Astrophys.* **2008**, *479*, 915.
[29] P. Lazaridis, G. Debarge, P. Gallion, *Opt. Lett.* **1995**, *20*, 1160.
[30] J. Shlens, *Int. J. Remote Sens.* **2014**, *5*, 2.
[31] A. A. Miranda, Y. Le Borgne, G. Bontempi, *Neural Process Lett.* **2008**, *27*, 197.

SUPPORTING INFORMATION

Additional supporting information may be found online in the Supporting Information section at the end of this article.

How to cite this article: Gagliardi S, Marrocco M, Rondino F, Palumbo D, Merla C, Falconieri M. Studies of supercontinuum generation in a photonic crystal fiber for use as Stokes beam in a single-laser femtosecond micro-CARS setup. *J Raman Spectrosc*. 2020;1–8. https://doi.org/10.1002/jrs.5897